

Contents lists available at ScienceDirect

## Acta Materialia

journal homepage: www.elsevier.com/locate/actamat



Full length article

# Lattice transformation in grain boundary migration via shear coupling and transition to sliding in face-centered-cubic copper



Bin Li\*, Janel Leung

Department of Chemical and Materials Engineering, University of Nevada, Reno, USA

#### ARTICLE INFO

Article history: Received 4 April 2021 Revised 21 June 2021 Accepted 22 June 2021 Available online 26 June 2021

Keywords: Grain boundary Shear coupling Sliding

#### ABSTRACT

Migration of symmetric tilt grain boundaries (GBs) via shear coupling has been studied extensively in experiments and simulations. It was reported that shear coupling transitioned to GB sliding at high temperatures, but how such transition occurs at low temperatures has not been investigated. Lattice transformation on the atomic scale during shear coupling has not been fully understood. In this work, mode of motion of symmetric tilt GBs with [001] tilting axis in face centered cubic copper under a shear strain parallel to the boundary plane at 100 K was carefully characterized by tracking the positions of the corresponding planes in atomistic simulations and new features of GB motion were observed. The results show that the angles between the two low-index planes, (110) and (100), and the boundary plane can be used to define a nominal magnitude of shear s. Approximately, if one of these two planes has a value of s < 0.5, shear coupling occurs with this plane being the active invariant plane; if 0.5 < s < 0.6, GB moves by shear coupling + sliding, i.e. a hybrid mode by which shear coupling transitions to sliding; if both planes have a value of s > 0.6, only GB sliding occurs. Careful structural analyses show that, for all the GBs that undergo shear coupling, some GB atomic planes remain invariant, very similar to the first invariant plane in deformation twinning, whereas the other GB atomic planes swap their positions in the GB normal direction through highly coordinated and complex atomic shuffles. This behavior allows identification of transformation units that are reoriented toward the neighboring grain. Rate-limiting factors are identified for lattice transformation and can be used to infer a kinetics model for shear coupling.

© 2021 Acta Materialia Inc. Published by Elsevier Ltd. All rights reserved.

### 1. Introduction

Grain boundaries (GBs) in crystalline materials play a crucial role in their physical and mechanical properties. How GBs, including high angle GBs (HAGBs) and low angle GBs (LAGBs) migrate under thermal and mechanical driving forces has been an important subject in physical metallurgy. Pioneering experimental works revealed GB migration under shear loading when a finite shear factor was present on the GB plane. Fukutomi and Kamijo [1] conducted observations on migration of  $\langle 110 \rangle \Sigma 11$  {113} symmetric tilt GBs in a bi-crystal aluminum (Al) sample. It was found that the pre-scribed scratches on the sample surface which served as fiducial markings became distorted as the GB position shifted. The distortion of the markings indicate that the GB migrates not only in parallel to the boundary plane, but also along the normal to the boundary plane, somewhat similar to migration of twin bound-

aries. The coupled migration was attributed to slip of GB dislocations [2]. Similar behavior was also observed in other experiments [3-12].

Cahn et al. [13] illustrated several scenarios that could occur when a shear strain was applied parallel to the GB plane of a coincident site lattice (CSL) [14]. One scenario is that, if a marker line is placed across the GB, this line will become distorted as the GB migrates upward as a result of shear coupling. Some GBs may also migrate downward by shear coupling under similar loading conditions, causing the marker line to be distorted in the opposite direction. Since the seminal work by Cahn et al. [13], shear coupling of symmetric tilt GBs and asymmetric tilt GBs has received significant attention and has been investigated in extensive atomistic [15-35] and phase field simulations [36,37]. Another scenario is that the GB stays roughly in the same position, but sliding of one grain relative to the other takes place (the GB may still migrate a little due to material transfer across the interface and this is the scenario of friction between two contacting surfaces [38]). Accordingly, the marker line inside one grain is translated along with GB sliding. It has been shown that shear coupling transitions to sliding

<sup>\*</sup> Corresponding author. E-mail address: binl@unr.edu (B. Li).

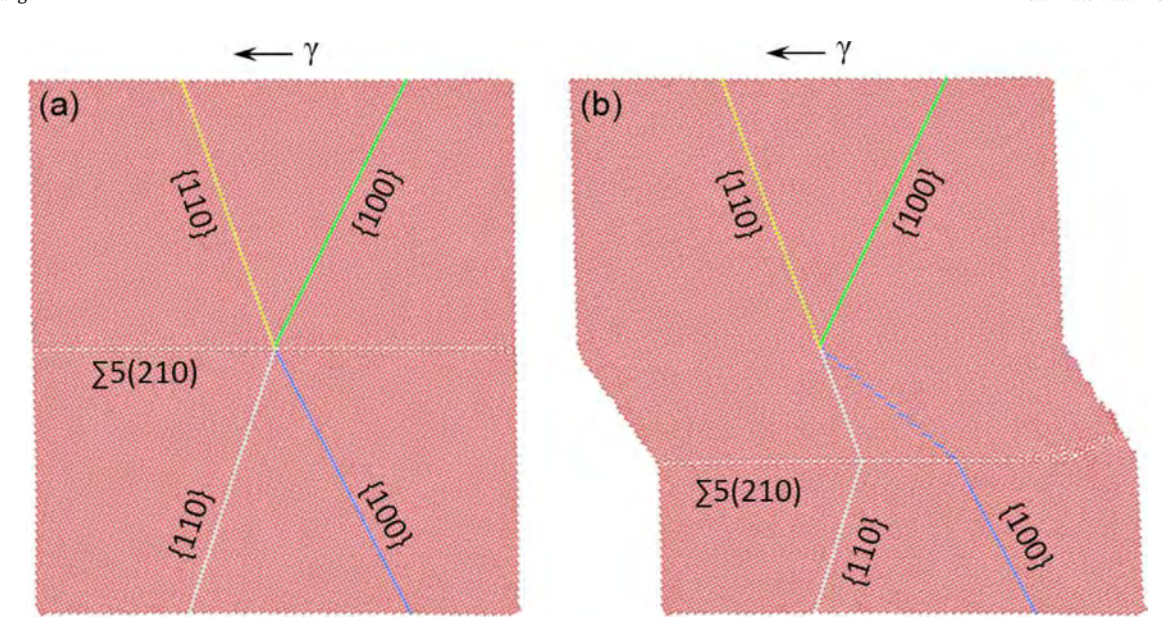


Fig. 1. (a) The relaxed initial configuration of a  $\Sigma$ 5(210) symmetric tilt GB. The {110} and {100} planes of the top and bottom grains are pre-selected and colored differently, in order to track the evolution of these planes. (b) The GB is migrating downward under the applied shear strain. Note that the white atoms of the {110} planes of the bottom grain are aligned to the {110} plane of the top grain, indicating that the {110} plane is the invariant plane.

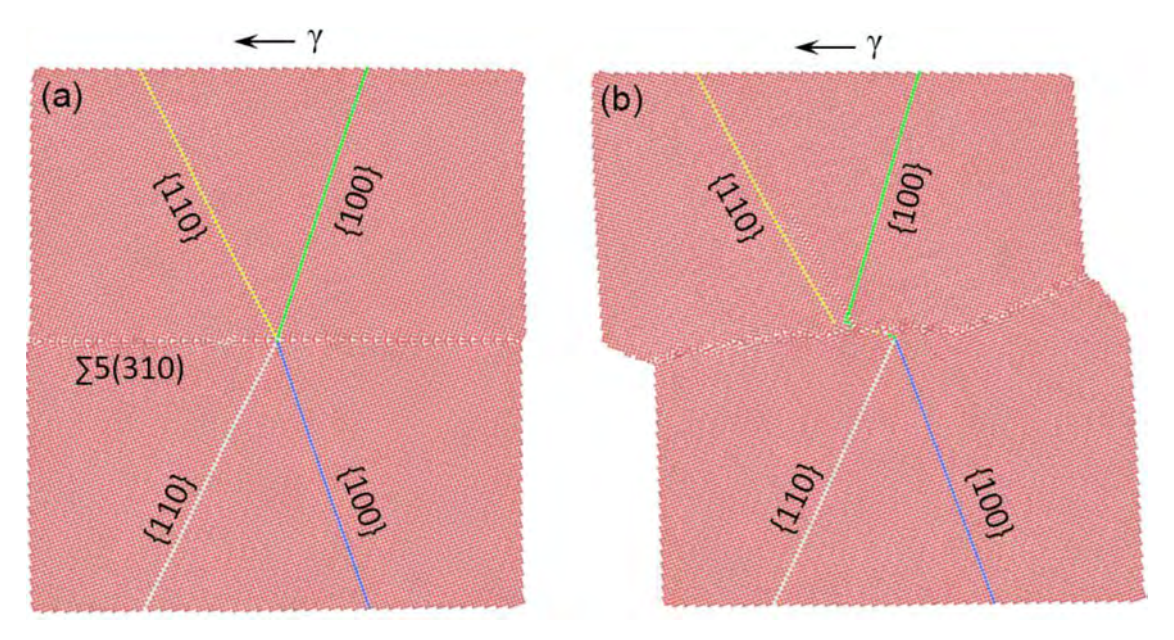
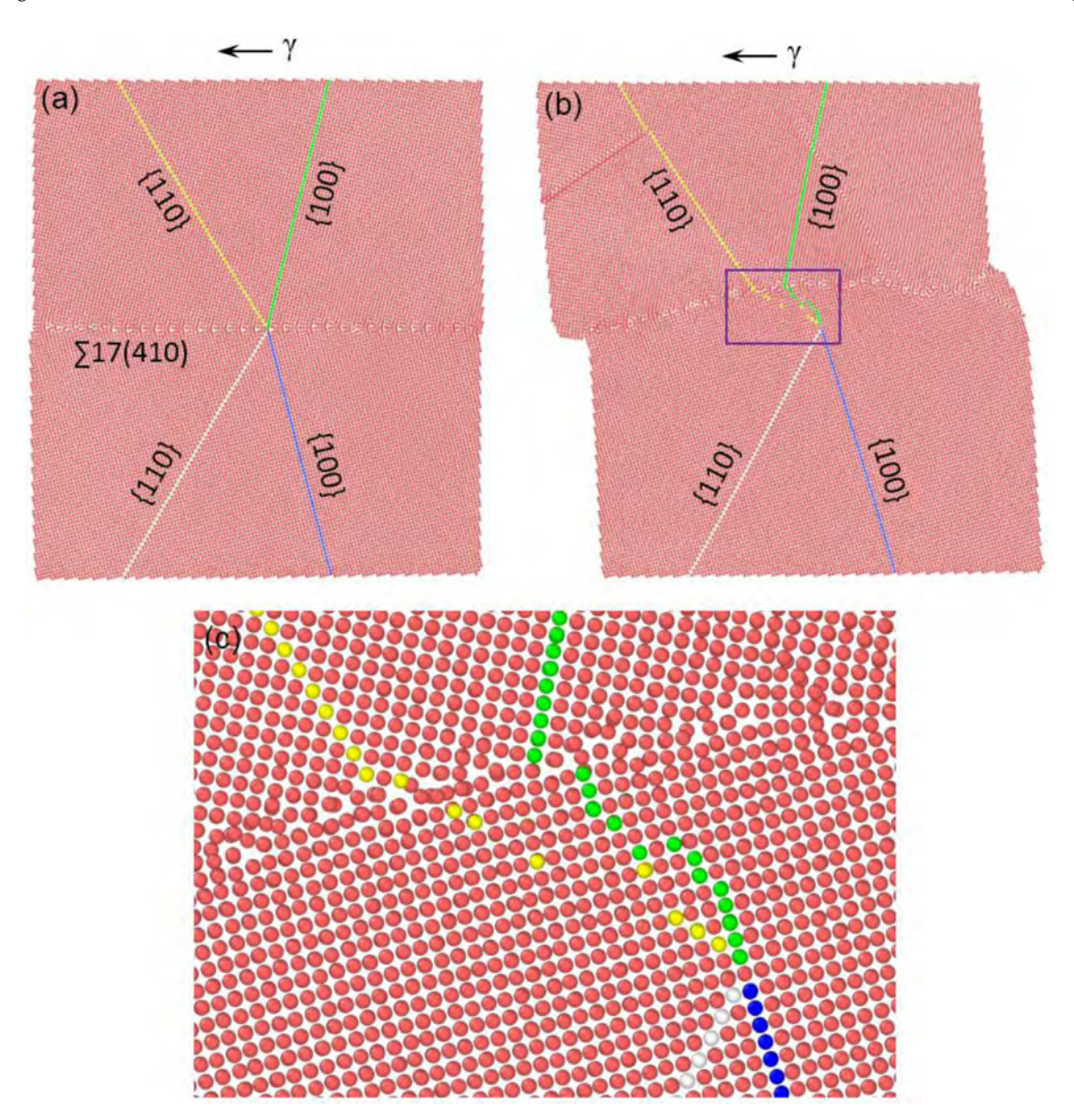


Fig. 2. (a) The relaxed initial configuration of a  $\Sigma$ 5(310) symmetric tilt GB. (b) The GB moves by sliding under the applied shear strain. No shear coupling occurs.

when the simulation temperature is sufficiently high [13,18]. However, there are indications that such transition may also occur at low temperatures [22], but the results in previous works did not reveal under what conditions shear coupling transitioned to sliding. Consequently, the mechanism that accounts for such a transition has not been understood.

Interestingly, a number of researchers noticed the similarity between migration of symmetric tilt GBs via shear coupling and migration of twin boundaries. Caillard et al. [39] proposed a geometrical model to describe the lattice transformation between two neighboring grains. In this model, two undistorted planes were defined, very similar to the first and second invariant plane defined in classical twinning theory [40]. For CSL GBs with [001] rotation axis, it was found that the second undistorted plane alternated between {100} and {110} as the misorientation angle varied [13,39]. Molodov et al. [7] recognized that the coupling factor was similar

to "magnitude of twining shear" defined in classical twinning theory, and they defined the coupling factor as "amount of shear", and developed a general formula to predict possible coupling factor or amount of shear by introducing a weighting factor for twin boundaries and GBs. Cahn et al. [13] pointed out that the GB plane could only be invariant on the macroscopic scale. Due to the presence of GB free volume, obviously some GB atomic planes cannot be maintained invariant in the sense that atomic shuffles that move in the GB normal direction must occur during migration via shear coupling. But other GB atomic planes may be indeed invariant as suggested by Caillard et al. [39] and Molodov et al. [7], because there is no volumetric dilation or contraction along the GB normal direction during migration. The existence of "undistorted planes" in shear coupling implies that the fundamental principle - lattice correspondence, which ubiquitously exists in migration of interphase boundaries in martensitic transformations and twin boundaries in



**Fig. 3.** (a) The relaxed initial configuration of a  $\Sigma$ 17(410) symmetric tilt GB. (b) The GB motion contains both sliding and shear coupling. (c) A magnified view of the boxed region in (b), showing a hybrid motion mode of shear coupling + sliding.

mechanical twinning [41–43] may also be applicable to GB migration via shear coupling. Partial lattice correspondence may still exist in shear coupling. To accurately describe the motion of a GB via shear coupling and how one lattice is transformed into the other, it is necessary to closely examine the evolution of GB atomic planes.

There have been extensive discussions of possible interfacial defects that mediate GB migration via shear coupling. It is known that for HAGBs, dislocations cannot be resolved on the GBs. However, Cahn et al. [44] argued that during migration of some CSL GBs via shear coupling, dislocation content could still be resolved because a finite shear was produced. A topological model, i.e. disconnections, has been widely used to describe GB motion [15,17,18,23]. Recently, Deng and Deng [17] reported nucleation and glide of disconnections on a  $\Sigma 5(210)$  GB. Their results show that shear coupling occur under shear strain, and a well-defined step, which is similar to a line defect, propagated on the GB plane. Chen et al. [15] reported that multiple disconnection modes conspired to move GBs in shear coupling. However, how these pro-

posed GB defects transform one lattice into the other while maintaining the lattice correspondence is not considered.

The purpose of this work is to provide novel analyses on structural evolution of CSL GBs with [001] tilting axis in various motion modes, i.e. shear coupling, sliding and transition between the two, in FCC copper (Cu) at 100 K, by using atomistic simulations. Special attention is paid to lattice transformation during shear coupling. The results obtained offer new insight on the nature of GB migration.

## 2. Simulation method

Initial Cu bi-crystals were constructed based on the coincidence site lattice (CSL) GB model [14]. The interatomic potential for pure Cu developed by Mishin et al. [45] was used for the simulations in this work. Two grains were rotated around the [001] tilting axis by the values of tilt angle that satisfied the definition of CSL GBs. Fig. 1a shows the relaxed initial configuration of a  $\Sigma$ 5(210) symmetric tilt GB. The system contains about 1.0 million atoms and

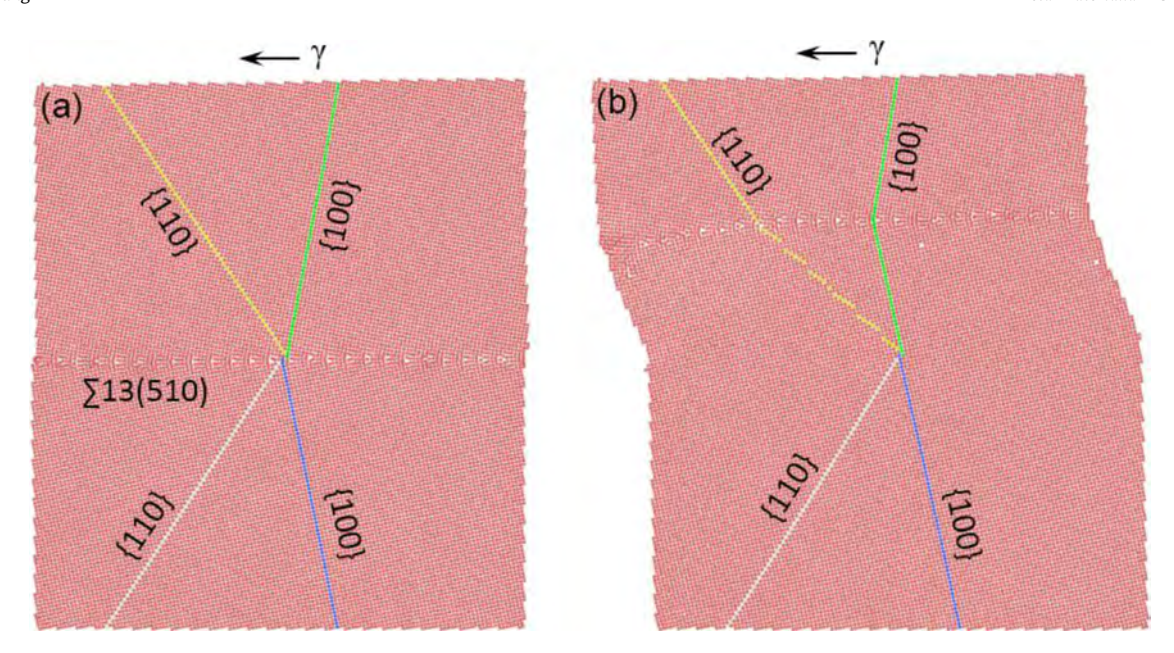


**Fig. 4.** (a) The relaxed initial configuration of a  $\Sigma$ 13(510) symmetric tilt GB. (b) The GB migrates upward by shear coupling. Note that the green atoms of the {100} planes of the top grain are being aligned to the {100} planes of the bottom grain, indicating that the {100} plane is now the invariant plane.

the size of the system box is 24  $\times$  26  $\times$  20 nm. Free surfaces were applied to all three dimensions. No periodic boundary condition was applied. Periodic boundary conditions were not used in our simulation systems because for such boundary conditions. atoms interact across the boundary. When lattice periodicity cannot be defined across the boundary, abnormal stress states at these boundaries would be generated and non-physical structures could occur. The temperature of the system was clamped at 100 K during simulation by applying the Nosé-Hoover thermostat [46,47]. A shear strain was applied to the system by constantly displacing (0.1 Å/ps) two layers of atoms on the top surface while another two layers of atoms on the bottom surface were fixed, corresponding to a strain rate of  $4.2 \times 10^8$  /sec. The system was relaxed for 50 ps before the external shear strain was applied. Simulation package for Large-Scale Atomic/Molecular Massively Parallel Simulation (LAMMPS) [48] was used for all the simulations and computations, i.e. potential energies and stresses, in this work.

Fig. 1a shows a crucially important feature in our simulations and analyses. The {110} and {100} planes of the top grain and the bottom grain were pre-selected and colored in yellow, green, white and blue, respectively. This color pattern was retained throughout the simulations. These colored atomic planes serve as marker lines so that we can unambiguously track the evolution of the lattices when the GB is migrating upward or downward. This technique was applied to the simulations of all types of GB systems in this work. The significance of why these two low-index planes were pre-selected will be seen in the simulation results as follows.

## 3. Results

Fig. 1b shows that the  $\Sigma$ 5(210) GB migrates downward under the shear strain. As the GB migrates, a salient feature can be observed. The white atoms, which reside on the pre-selected {110} plane of the bottom grain, are being aligned to the yellow, pre-selected {110} plane of the top grain. In contrast, the {100} plane of the bottom grain (the blue atoms) is transformed to a different plane (close but not exactly the {100} plane) of the top grain, as seen from the broken blue trace. This behavior is called "lattice correspondence", meaning that an atomic plane of one lattice must be transformed or mapped to a corresponding plane of the product

lattice and such a correspondence is unique for a specific transformation. Thus, in this particular case, an invariant plane, which is the {110} plane, can be identified. The definition of this invariant plane is similar to the "second invariant plane" [49,41] in deformation twinning. As shown in the following, this invariant plane is not exclusive and can switch to the {100}, depending on the misorientation angle of GB.

For the  $\Sigma$ 5(310) GB, the scenario of GB motion under the shear strain is completely different from the  $\Sigma$ 5(210) GB, as shown in Fig. 2. Although the relaxed initial GB is nearly coherent (Fig. 2a), under the shear strain, the coherent GB becomes rough and incoherent and the top grain is sliding against the bottom one. The position of the GB almost remains at the same position. The displacement produced by GB sliding can be clearly seen from the large steps on the free surfaces and the translation of the marker lines. Obviously, a transition from shear coupling for  $\Sigma$ 5(210) to GB sliding for  $\Sigma$ 5(310) takes place for some reason that will be explored and discussed below.

As we change the GB type to  $\Sigma$ 17(410) (Fig. 3a), again, GB sliding occurs (Fig. 3b). However, the sliding is quite different from the sliding in  $\Sigma$ 5(310) in that shear coupling actually also occurs as the sliding is occurring. In other words, shear coupling and GB sliding occurs concomitantly. This can be seen from the fact that some green atoms, which reside on the pre-selected {100} plane of the top grain, are aligned to the blue {100} plane of the bottom grain; but the alignment is disrupted by GB sliding. The boxed region in Fig. 3b is magnified and shown in Fig. 3c. The green atoms are intermittently aligned to the blue {100} plane of the bottom grain. This fact clearly indicates that for this  $\Sigma$ 17(410) GB, shear coupling and GB sliding occur simultaneously under the external shear strain, i.e. a hybrid mode of motion is present.

As we continue to change the GB type to  $\Sigma 13(510)$  (Fig. 4a), the motion of this GB is again dominated by shear coupling (Fig. 4b). However, an outstanding difference in this particular scenario is that the invariant plane is now shifted to {100}. It can clearly be seen that the green atoms which originally reside on the {100} plane of the top grain, are now aligned to the blue {100} plane of the bottom grain. As a result, the GB is migrating upward, if we compare Fig. 4 with Fig. 1 which is the shear coupling of  $\Sigma 5(210)$  moving downward.

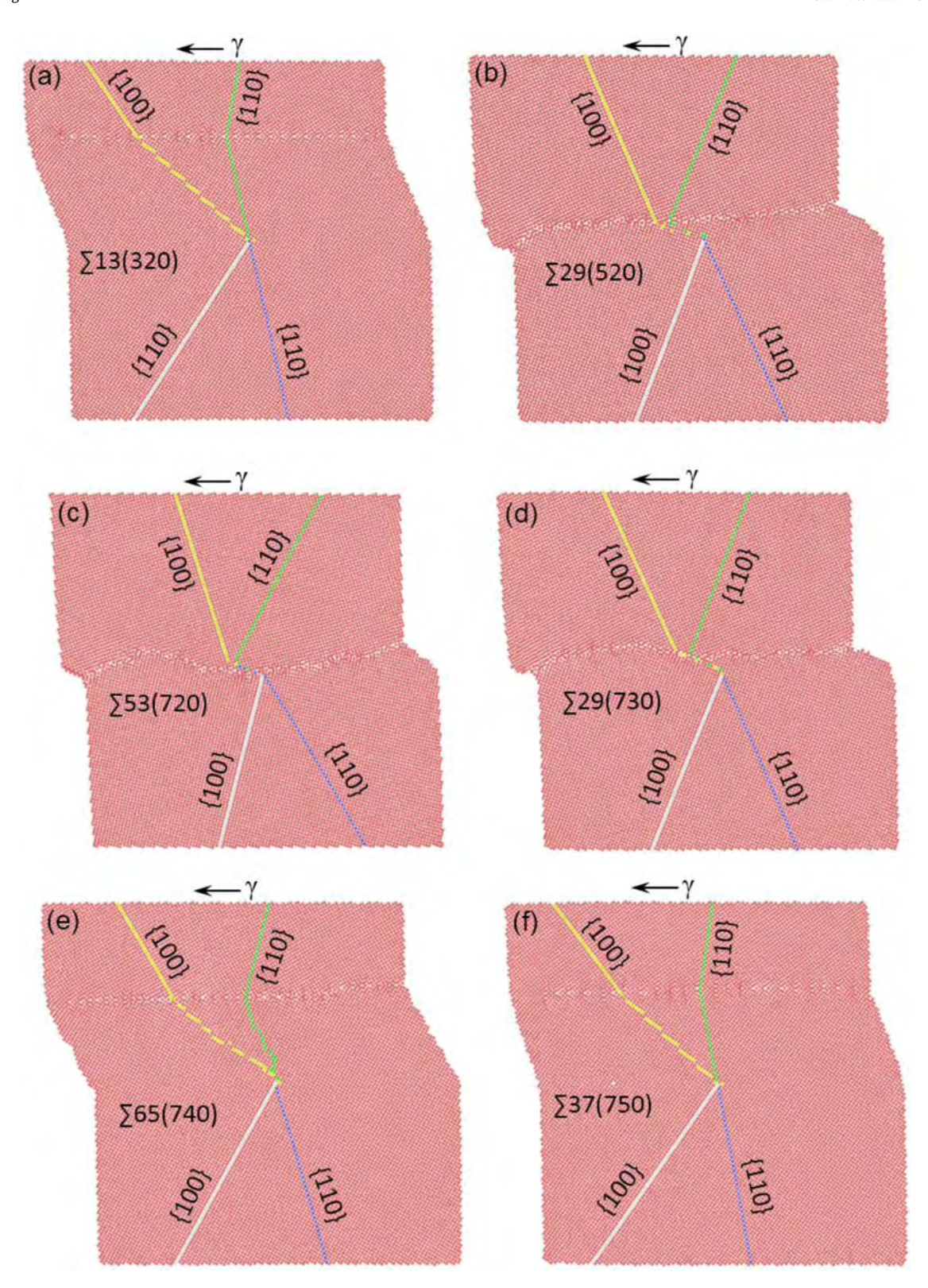


**Fig. 5.** (a) Shear coupling of a  $\Sigma$ 13(320) GB. The invariant plane is {110}. (b) GB sliding of  $\Sigma$ 29(520). (c) GB sliding of a  $\Sigma$ 53(720). (d) GB sliding of  $\Sigma$ 29(730). (e) Shear coupling + sliding of  $\Sigma$ 65(740). Shear coupling is the major component. (f) Shear coupling of  $\Sigma$ 37(750). The invariant plane is the {110}.

Figs. 1 to 4 demonstrate an important behavior that, as we change the GB type from  $\Sigma5(210)$  to  $\Sigma5(310)$ , and to  $\Sigma17(410)$ , and then to  $\Sigma13(510)$ , under the same loading condition, the GB motion transitions from shear coupling with {110} being the invariant plane, to GB sliding, and to hybrid shear coupling + slid-

ing, and then to shear coupling with  $\{100\}$  being the invariant plane. Accordingly, the switch from invariant  $\{110\}$  to invariant  $\{100\}$  causes the GB motion to switch direction from downward to upward.

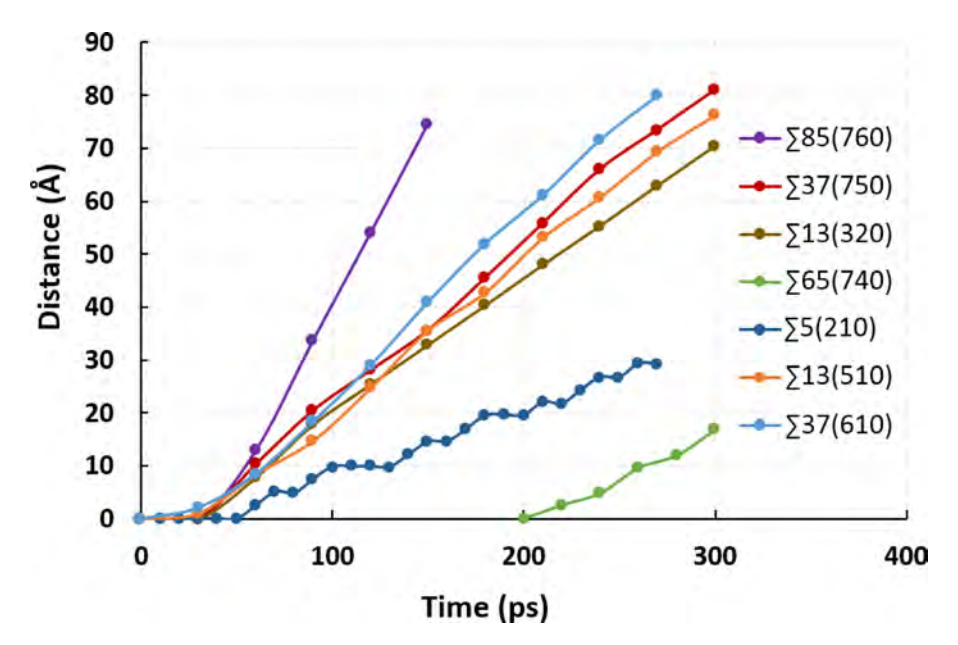


Fig. 6. The displacement of GB motion in the vertical direction against simulation time. The slope is the  $v_{\perp}$  of the symmetric tilt GBs.

In order to confirm that the observed transitions of GB motion mode are universal and not an isolated case, we performed a series of similar simulations on other types of symmetric tilt GBs. The results are shown in Fig. 5. Fig. 5a shows the result from  $\Sigma$ 13(320). Clearly, shear coupling occurs and the invariant plane is {110}. For  $\Sigma$ 29(520),  $\Sigma$ 53(720) and  $\Sigma$ 29(730) (Fig. 5b to d), GB sliding dominates the GB motion. Until  $\Sigma$ 65(740), the GB motion transitions to shear coupling; however, GB sliding is also occurring simultaneously and this can be seen from the broken green {110} plane that are aligned to the blue {110} of the bottom grain. Thus, for  $\Sigma$ 65(740), the mode of motion is shear coupling + sliding but shear coupling is the major component. As we change the GB type to  $\Sigma$ 37(750), the GB motion is purely shear coupling without sliding and the invariant plane is {110}.

Despite the similar loading conditions for all the symmetric tilt GBs in the present work, the velocity of migration of individual GBs as a result of shear coupling varies significantly. We carefully measure the migration velocities by measuring the position of the colored atom that is located at a position where the line distortion occurs at that particular time step, and the vertical distance of GB migration is calculated in reference to the initial GB position. Thus, the measured velocity is the component in the vertical direction to the GB plane  $(\nu_{\perp})$ . The displacement of migration by shear coupling of the GBs are plotted in Fig. 6. Note that for  $\Sigma 37(740)$ , the shear coupling is disrupted by GB sliding, so only the displacement during a time period in which shear coupling is undisrupted is measured and plotted. Also, in Fig. 6, the displacements are plotted regardless of the moving direction of the GB. The steady state slope of individual curves represents the velocity of GB migration.

The velocities of motion driven by shear coupling can be divided into three ranges. At the low end are  $\Sigma5(210)$  and  $\Sigma37(740)$  which is disrupted by sliding. Among all the GBs that are simulated in this work,  $\Sigma5(210)$  is the one that presents a well-defined cyclic, "jerky" or stick-slip feature [50] in displacement. The structure of  $\Sigma5(210)$  and the mechanism for the observed migration characteristic will be analyzed in detail below. Both  $\Sigma5(210)$  and  $\Sigma65(740)$  migrate in a sluggish manner. At the high end,  $\Sigma85(760)$  migrates at the fastest velocity. The tilt angle of  $\Sigma85(760)$ , which equals ~9°, falls in the range of low angle grain boundaries (LAGBs). In the intermediate velocity range are  $\Sigma37(610)$ ,  $\Sigma37(750)$ ,  $\Sigma13(510)$  and

 $\Sigma13(320)$  in the order from high to low, but these GBs are all mobile

## 4. Analysis and discussion

4.1. Choice of the invariant plane and transition from shear coupling to sliding

The simulation results in this work show an important feature during migration of symmetric tilt GBs via shear coupling an invariant plane can be defined, as discussed by Caillard et al. [39] and Molodov et al. [7]. Cahn and Taylor [51] developed a unified approach for GB motion, in which they recognized that coupled GB migration under a shear strain parallel to the GB plane was similar to a simple shear. A special case of simple shear is deformation twinning in which most twin boundaries are highly coherent and thus can be treated as symmetric tilt GB as well. In a simple shear of twinning, atoms on the twinning plane, aka the first invariant plane, undergo a homogeneous shear along the twinning direction. The shear displacement of each twinning plane is proportional to the distance of that twinning plane to the position of the twin boundary. It is important to note that the shear displacement in deformation twinning is determined by the choice of the second invariant plane [41,52]. But the choice of the second invariant plane is restricted by several rules in terms of the magnitude of twinning shear and the complexity of atomic shuffles [41,52]. Naturally a question arises: in general, does shear coupling of symmetric tilt GBs obey these rules as well?

For the specific symmetric tilt GBs with a tilting axis of [001] in FCC metals, this invariant plane switches between two low-index planes, i.e. {110} and {100}, when the tilt angle between the two grains varies. As mentioned above, a highly coherent twin boundary created in deformation twinning can be treated as a special type of symmetric tilt GBs. In deformation twinning, two invariant planes can be defined: the first invariant plane or the  $K_1$  plane. This  $K_1$  plane is the twinning plane on which a homogeneous simple shear takes place and such a shear deformation is generally mediated by twinning dislocations [41,49,52]. The second invariant plane is called the  $K_2$  plane. It is important to note that the  $K_2$  plane defines the magnitude of twinning shear. It is this second invariant plane that determines the magnitude of the Burg-

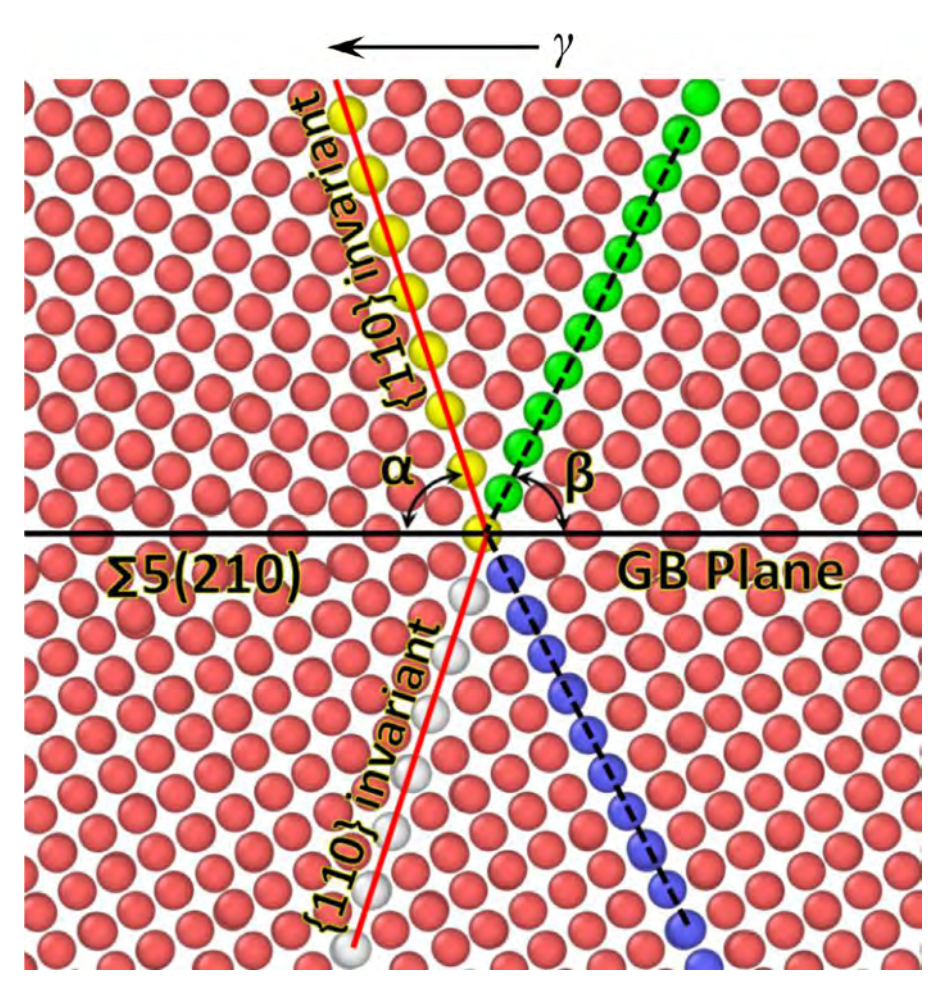


**Fig. 7.** Magnified view of the relaxed initial configuration of a  $\Sigma$ 5(210) GB. The {110} and {100} planes of the top and bottom grains are pre-selected and colored in yellow, white, green and blue, respectively. The magnitude of the two angles  $\alpha$  and  $\beta$  plays a crucial role in determining the mode of GB motion.

ers vector of twinning dislocations. According to Bilby and Crocker [49] and Christian [52], the choice of the second invariant plane should obey a few empirical rules. The first rule is that the magnitude of twinning shear should be as small as possible, and the second rule is that atomic shuffles should be as simple and small as possible. Preferably the atomic shuffles should be along the direction of the twinning shear. However, in deformation twinning, these two rules work at odds with each other. If the magnitude of twinning shear of a twinning mode is so small that large and complex atomic shuffles are incurred, the choice of the  $K_2$  plane may not be favorable and this is the case for  $\{11\overline{2}2\}\langle11\overline{2}\overline{3}\rangle$  twinning mode which has been observed in Ti and Zr [41,53,54]. The predicted  $K_2$  plane  $\{11\overline{24}\}$  in the classical twinning theory is likely incorrect because very complex atomic shuffles would be needed. In general, a small magnitude of twinning shear results in complex atomic shuffles. For all the deformation twinning modes, it was suggested that the magnitude of twinning shear should always be less than 1.0 [41,52].

In the following, we show that the observed GB behavior in this work generally obey these rules in the classical twinning theory. First, we examine the geometry of individual GBs and take  $\Sigma 5(210)$  as an example. A magnified view of this GB is shown in Fig. 7. The GB plane is indicated by the black line. The red lines mark out the traces of the  $\{110\}$  planes of the two neighboring grains and the atoms on these two planes are colored in yellow and white. The dashed black lines represent the traces of the  $\{100\}$  planes of the two grains and atoms on these two planes are colored in green and blue. Two important parameters can be defined in this GB ge-

ometry – the angle between the {110} plane and the GB plane designated as  $\alpha$ ; and the angle between the {100} plane and the GB plane designated as  $\beta$ . These designations are kept in the analyses hereafter. When the {110} is the invariant plane, the magnitude of shear (s) is designated as  $s_{\{110\}}$ ; when the {100} is the invariant plane, the magnitude of shear is designated as  $s_{\{100\}}$ . From the geometrical relationship, we have:

$$\alpha + \beta = \frac{3}{4}\pi\tag{1}$$

If the {100} is the invariant plane, then [13]

$$s_{\{100\}} = 2\tan\left(\frac{\pi}{2} - \beta\right) \tag{2}$$

If the {110} is the invariant plane, then [13]

$$s_{\{110\}} = 2\tan\left(\frac{\pi}{2} - \alpha\right) = 2\tan\left(\beta - \frac{\pi}{4}\right) \tag{3}$$

As s is defined by the invariant plane of  $\{110\}$  or  $\{100\}$  in the above equations, we can now calculate the value of s for all the GBs constructed in this work and the results are summarized in Table 1.

From the data in Table 1, it can clearly be seen that, shear coupling occurs to those GBs with s below 0.5 (approximately), irrespective of the invariant plane. In general, if one of the two planes has s below 0.5, then this plane with a low value of s will be the active invariant plane when shear coupling occurs. This indicates that, in Fig. 7, if we rock the positions of the {110} and {100} planes indicated by the solid red and the dashed black lines around

**Table 1**Summary of GB geometry and motion mode.

	α-(110) (deg.)	$\beta$ -(100) (deg.)	S	GB Motion Mode	
Σ5(210)	71.6	63.4	0.67	Mixed	
$\Sigma 5(310)$	63.4	71.6	0.67	Sliding	
$\Sigma 17(410)$	59.0	76.0	0.50	Hybrid: sliding + Shear coupling	
$\Sigma 13(510)$	56.3	78.7	0.40	Shear coupling	
$\Sigma$ 37(610)	54.5	80.5	0.33	Shear coupling	
$\Sigma 13(320)$	78.7	56.3	0.40	Shear coupling	
$\Sigma 29(520)$	66.8	68.2	0.80	Sliding	
$\Sigma 53(720)$	60.9	74.1	0.57	Sliding	
$\Sigma 29(730)$	66.8	68.2	0.80	Sliding	
$\Sigma 65(740)$	74.7	60.3	0.55	Hybrid: Shear coupling + sliding	
$\Sigma 37(750)$	80.5	54.5	0.33	Shear coupling	
$\Sigma 85(760)$	85.6	49.4	0.15	Shear coupling	

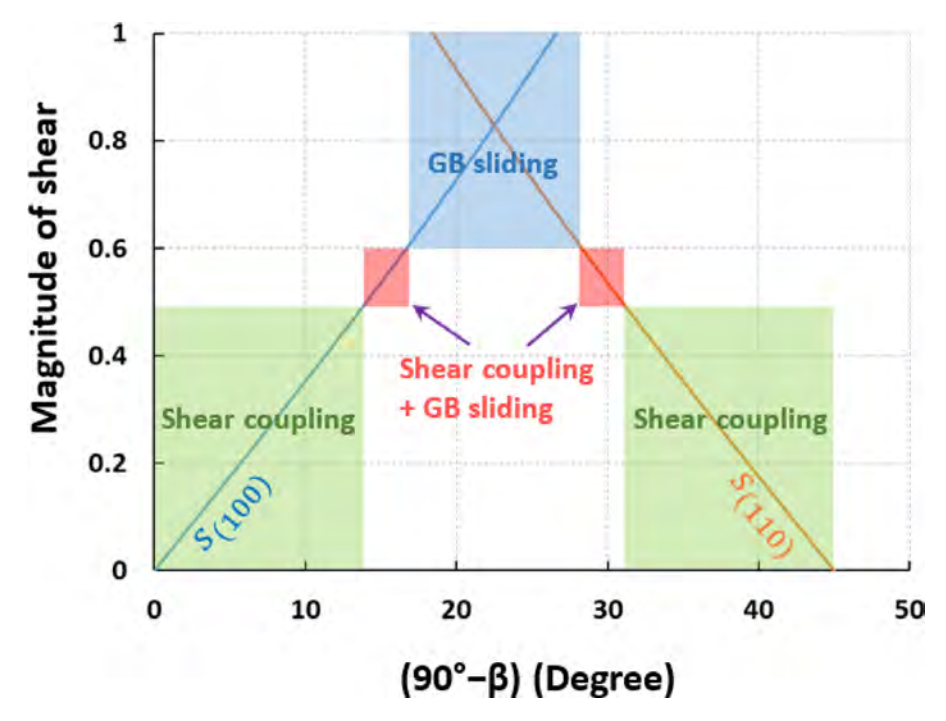


**Fig. 8.** Correlation between the magnitude of shear s and GB motion mode. The two curves are for the values of s when the invariant plane is  $\{100\}$  or  $\{110\}$  vs. the angle of  $(90^{\circ} - \beta)$ . Approximately, when s < 0.5, shear coupling dominates; when 0.5 < s < 0.6, shear coupling transitions to GB sliding; when s > 0.6, GB sliding dominates.

the tilting axis [001], the value of  $\alpha$  and  $\beta$  changes accordingly and continuously. If we rock the two atomic planes to the left, the value of  $\beta$  increases whereas the value of  $\alpha$  decreases. Accordingly,  $s_{\{100\}}$  decreases and  $s_{\{110\}}$  increases. According to the rules of the classical twinning theory, the  $\{100\}$  plane will become increasingly favorable to be the invariant plane. If we rock the two atomic planes to the right, the value of  $\beta$  decreases whereas the value of  $\alpha$  increases. Accordingly,  $s_{\{100\}}$  increases and  $s_{\{110\}}$  decreases, and thus the  $\{110\}$  plane will become increasingly favorable to be the invariant plane. This explains well the observed transition from the  $\{110\}$  invariant to the  $\{100\}$  invariant as we change the GB type from  $\Sigma 5(210)$  to  $\Sigma 5(310)$ ,  $\Sigma 17(410)$  and  $\Sigma 13(510)$  (Fig. 1 to 5).

For those GBs with s between 0.5 and 0.6 (approximately), the GB motion mode is hybrid of shear coupling and sliding, and these GBs are  $\Sigma$ 17(410) and  $\Sigma$ 65(740). For those GBs with s greater than 0.6 (approximately) for both {110} and {100}, only GB sliding occurs because neither of these two planes, i.e. {110} and {100} can become the invariant plane.

If we plot  $s_{\{110\}}$  and  $s_{\{100\}}$  Eq. (2) and (3) as a function of  $(90^{\circ} - \beta)$ , as shown in Fig. 8, the transition from shear coupling to GB sliding can be well resolved. Only those values of s lower than 1.0 are plotted in Fig. 8. The plot area can be divided into sub-areas

based on the value of s and accordingly the range of tilt angles. For  $s_{\{110\}}$  and  $s_{\{100\}}$ , whichever is the smaller and below 0.5, shear coupling will dominate GB migration. As s increases, shear coupling transitions to GB sliding. In a small range of 0.5 < s < 0.6, GBs migrate in a hybrid mode of shear coupling + sliding. As s further increases to greater than 0.6 for both {110} and {100}, within the corresponding range of tilt angles, GB sliding dominates without shear coupling. Although the values of  $(90^{\circ} - \beta)$  only covers 0 ~ 45°, i.e.  $\beta$  falls between 45° ~ 90°, Fig. 8 actually covers the whole range from 0 to 90° of  $\beta$  or  $\alpha$ , this is because the {110} bisects the angle between the  $\{100\}$  and  $\{010\}$ . If  $\beta$  of  $\{100\}$  is larger than 45°, then the tilt angle of {010} is smaller than 45°, but {100} and  $\{010\}$  are crystallographically equivalent. The  $v_{\perp}$  velocity component of GB migration when shear coupling dominates can be plotted against s, as shown in Fig. 9. It can be seen that  $v_{\perp}$  is a strong function of s. In general, smaller values of s produce faster migration velocities than do large values.

The rules of the classical analyses by the pioneers in deformation twinning explain well the observations in this work and the other works. First, the two low-index planes, i.e. {110} and {100}, have always been observed in GBs over high-index atomic planes as the invariant plane. This is because that, the number density of

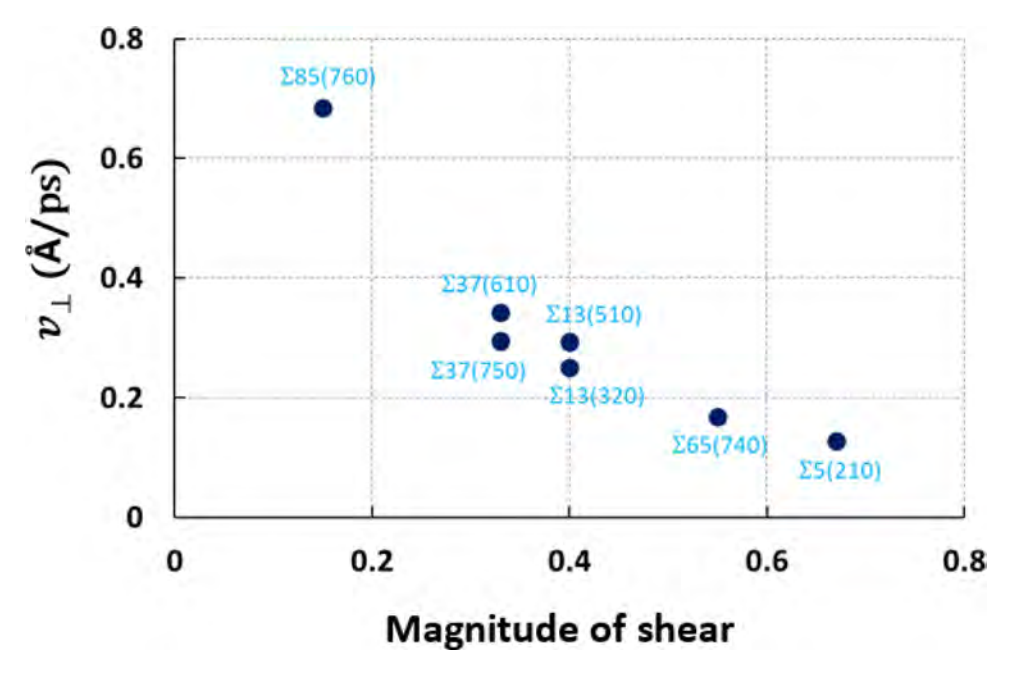


Fig. 9. The vertical velocity component  $v_{\perp}$  of GB motion of the symmetric tilt GBs as plotted against the magnitude of shear (s).

atoms on these two planes are higher than other atomic planes with the same tilting axis of [001]. When one of these two low-index planes is the active invariant plane, the number of atoms that are directly sheared to the lattice of the neighboring grain will be maximal, and the shuffles that are required for the other atoms will be relatively simple. Thus, the symmetric tilt GBs with a tilting axis of [001] always choose either {110} or {100} as the invariant plane, as shown in Fig. 1 to 5. Second, a GB with a small value of *s* is more likely to migrate via shear coupling and the migration velocity is faster (i.e. a higher mobility) than a GB with a larger *s*. This is because a small *s* and relatively simple shuffles are always preferred, according to the classical twinning theory. This trend is generally consistent with the results reported by Cahn et al. [13] and Homer et al. [20].

It is seen that  $\Sigma 5(210)$  is the only exception to the otherwise perfect correlations that have been discussed thus far. This GB has s of 0.67 ( $\alpha = 71.6^{\circ}$ ) which is fairly large, but shear coupling still occurs. For other GBs that have similar s, such as  $\Sigma 5(310)$  $(\beta = 71.6^{\circ})$ , only sliding occurs. From the velocity plots (Fig. 6 and 9),  $\Sigma 5(210)$  has the slowest migration velocity, even slower than that of  $\Sigma 65(740)$  ( $\alpha = 74.7^{\circ}$ ) in which shear coupling is disrupted by GB sliding. Careful examination of the simulation results reveals that the  $\Sigma$ 5(210) actually moves in a mixed mode. Fig. 10a shows common neighbor analysis (CNA) [55] of the simulation results. The viewing direction is along the direction of the external shear strain, i.e. a side view. Atoms on the GB (plotted in white) have different common neighbor values than those atoms on the perfect FCC lattice that are plotted in green. It can clearly be seen that, during GB motion, only the middle portion of the GB undergoes shear coupling, whereas the two regions away from the middle undergo sliding but the boundary plane is no longer the original GB plane. Fig. 10b shows a 3D view of the  $\Sigma$ 5(210) GB in which the green atoms are removed. The middle portion that undergoes shear coupling remains coherent. A step can be well resolved in the middle region. This step behaves like a dislocation line traversing the middle GB portion and driving the GB migration. In contrast, outside the middle region toward the free surfaces, the GB structure is rather disordered as a result of GB sliding.

To better resolve the transition in the mixed motion mode of the  $\Sigma 5(210)$  GB, multiple thin slices (0.5 nm in thickness) that are

perpendicular to the figure plane of Fig. 10a are taken from the middle region of Fig. 10a toward the right free surface, and the configurations are shown in Fig. 11. It is clear that in the middle region, shear coupling dominates the GB motion. But as the slicing moves away from the middle toward the surface, more and more GB sliding is mixed in the motion. Near the surfaces, the motion is dominated by GB sliding. This can be seen from the increasing translational distances of the white and blue planes in the bottom grain in reference to the yellow and green atoms in the top grain.

In the following, how lattice transformation is accomplished during GB migration via shear coupling is analyzed in detail.

## 4.2. Lattice transformation units in shear coupling

The fact that during shear coupling, the GBs, irrespective of their CSL structure, the migration front always maintains planar indicates that some GB atomic planes remain almost on the same vertical positions. Thus, these atomic planes can be considered as invariant too, just similar to the first invariant plane in deformation twinning. To demonstrate this crucial characteristic in GB migration, examples of  $\Sigma 5(210)$  and  $\Sigma 13(320)$  are analyzed, as shown in Fig. 12a and b, respectively. The  $\Sigma 5(210)$  GB (denoted by the solid black line in Fig. 12a) migrates downward with the {110} being the invariant plane. It can be seen that the {110} invariant plane intersects every third (210) plane (denoted by the horizontal dashed black line) at a lattice point which is denoted by the black dots. During GB migration, the vertical positions of these (210) planes almost remain unchanged (minor changes may occur due to relaxation after shuffling), and they are transformed to the (210) planes of the top grain. This process is very similar to the first invariant or  $K_1$  plane in deformation twinning, which requires any vector in this plane retain its original direction and magnitude. In deformation twinning of low symmetry crystal structures such as hexagonal close-packed (HCP) metals, migration of some twin boundaries is mediated by "zonal twinning dislocations" [41,56,57]. The height of a zonal twinning dislocation is defined by the number of twinning planes that are comprised between the twin boundary and the plane intersecting the second invariant plane at a lattice point [56,58,41]. Atoms at these intersections are directly sheared to the twin lattice without the need

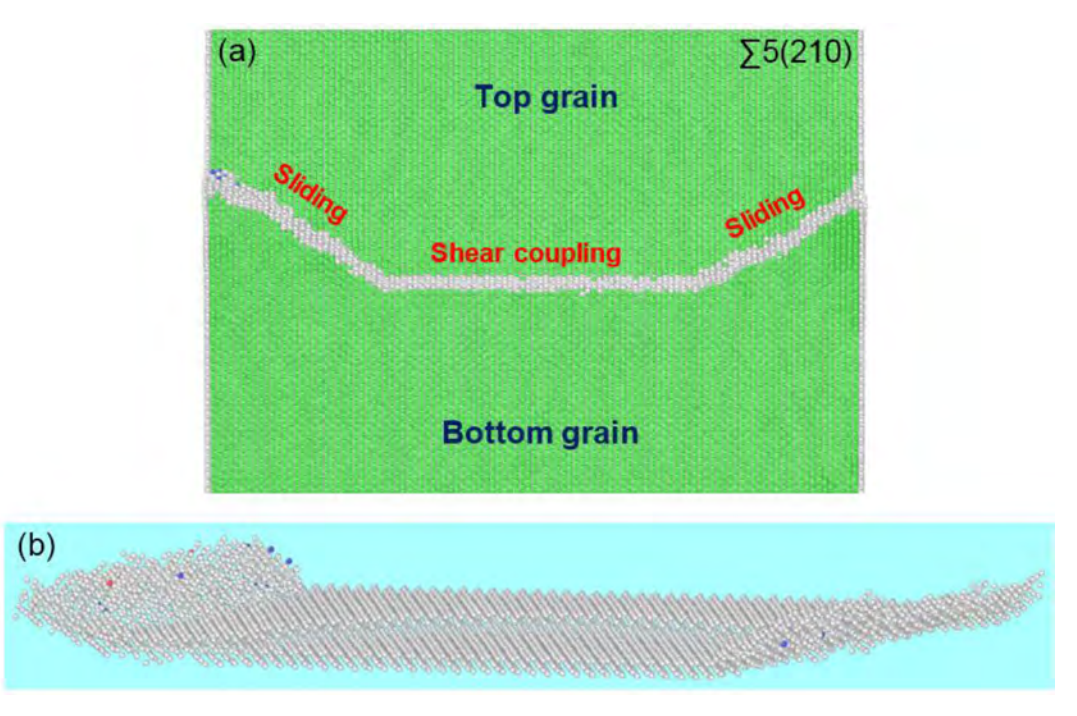


**Fig. 10.** (a) Side view (along the shear direction) of the mixed  $\Sigma$ 5(210) GB motion. Only the middle region of the GB undergoes shear coupling, whereas the regions near the free surfaces undergo sliding. (b) 3D view of the moving  $\Sigma$ 5(210) GB. The green atoms of FCC in (a) are removed. A step in the middle region can be observed.

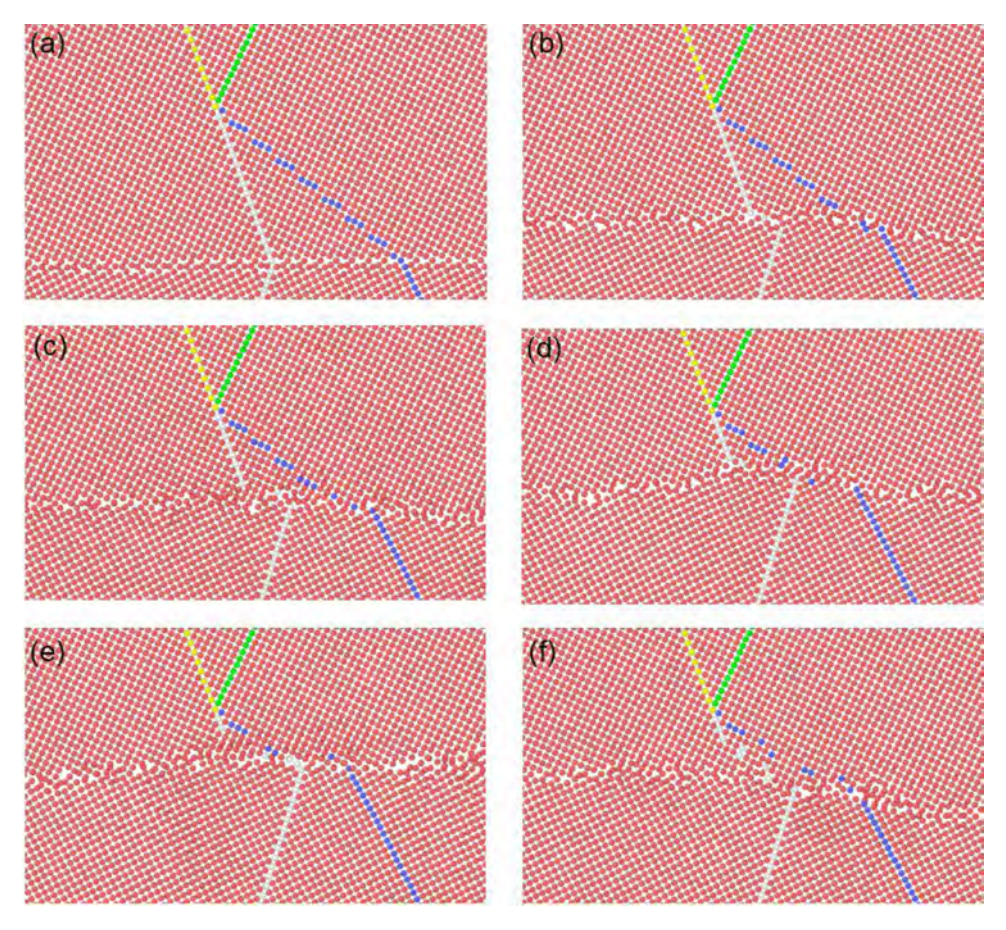
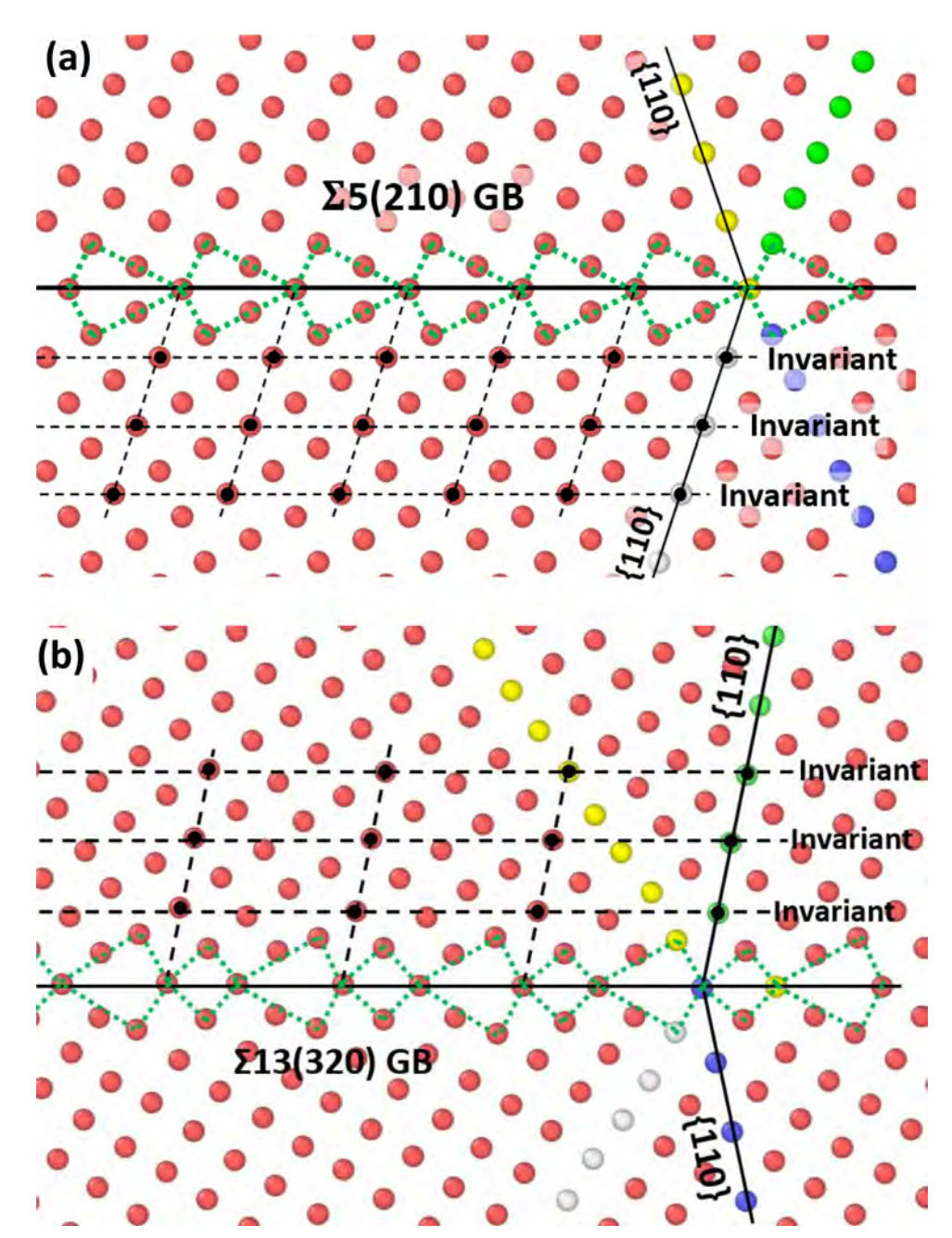


Fig. 11. Transition from shear coupling to sliding from the center of the system toward the free surface in the simulation of the  $\Sigma$ 5(210) GB at a fixed time step. A series of thin slices that are perpendicular to the figure plane of Fig. 9a are taken from the center toward to the right free surface. In the center region, i.e. (a), shear coupling dominates. Close to the surfaces, i.e. (f), GB sliding dominates.



**Fig. 12.** (a) Definition of lattice transformation units in  $\Sigma$ 5(210). Starting from the GB plane (denoted by the solid black line), every third (210) intersects the {110} at a lattice point (denoted by the black dots), and these intersecting (210) planes remain nearly on the initial level when the GB passes through (see Fig. 13 below). Thus, they can be considered as "invariant planes", analogous to the first invariant plane in deformation twinning. The rest of the atoms undergo highly coordinated shuffles during GB migration via shear coupling. (b) Transformation units in  $\Sigma$ 13(320). Every fifth (320) intersects the {110} at a lattice point. The dotted green lines delineate the GB structural

of shuffling. A similar analysis is presented for  $\Sigma 13(320)$  (Fig. 12b) in which every fifth (320) plane intersects the {110} invariant plane at a lattice point. As shown below, the individual parallelepipeds outlined in Fig. 12 can be defined as "transformation units" that transform the lattice of one grain into the lattice of the neighboring grain.

To find out how the lattice of a grain is transformed into the lattice of the neighboring grain, it is necessary to closely examine how the other GB atomic planes move during shear coupling. For this purpose, four layers of consecutive (210) planes of the bottom grain are pre-selected and colored in red, blue, green and cyan (Fig. 13a(i)). This color pattern is retained during GB migration via shear coupling. A very interesting feature in this analysis is that,

as the GB is passing through the pre-selected region, the blue and green atoms are swapping their positions in the GB normal direction (Fig. 13a(ii)), in contrast to the red and cyan layers that are almost invariant. The highly coordinated atomic shuffles gradually change the orientation of individual units in the bottom grain toward the orientation of the top grain. Eventually, after the GB passes through the pre-selected region, the transformation units complete their reorientation (Fig. 13a(iii)). Most interestingly, after reorientation, each colored (210) plane remains single colored, i.e. the green atoms remain on the same (210) plane and so do the blue atoms. In other words, the lattice transformation is accomplished by swap of positions of those (210) planes that are not

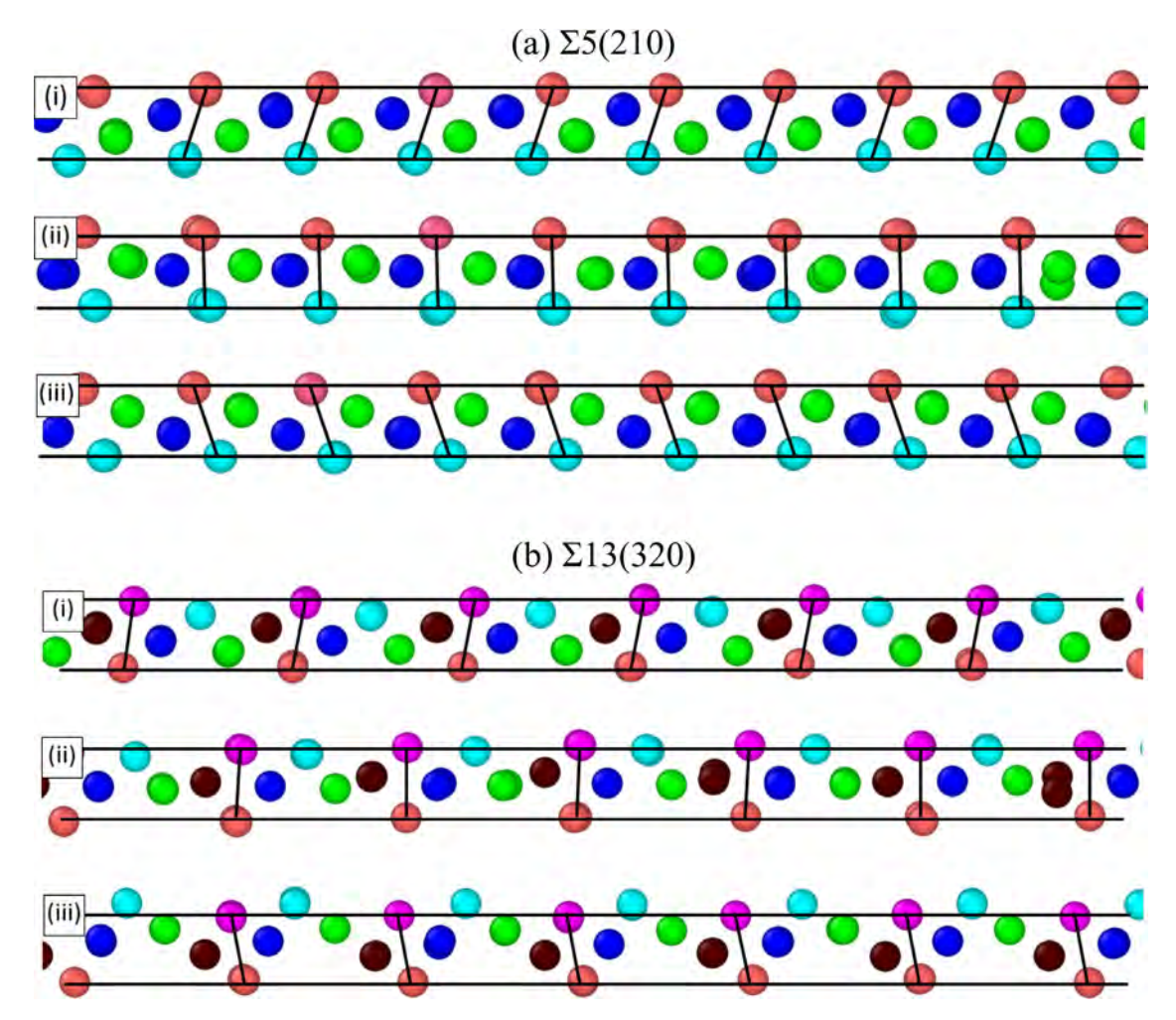


Fig. 13. Evolution of transformation units during shear coupling. (a)  $\Sigma$ 5(210). Consecutive (210) planes are pre-selected and colored in red, blue, green and cyan. Transformation units are outlined by the black lines. During shear coupling, the transformation units are reorienting by highly coordinated shuffles such that the green and the blue (210) planes are swapping positions in the vertical direction. Meanwhile, the red and cyan (210) planes remained nearly at the initial levels. After the completion of reorientation, each (210) plane remains single colored, i.e. atoms of each (210) plane remain on the same (210) plane. (b)  $\Sigma$ 13(320). Consecutive (320) planes are selected and colored differently. During shear coupling, non-invariant (320) planes swap positions by highly coordinated shuffles. After reorientation, each (320) plane remains single-colored, i.e. atoms on each (320) plane remain on the same (320) plane, despite the complex shuffles.

invariant in the GB normal direction, via highly coordinated and complex shuffles.

Similar lattice transformation behavior can also be observed in all other CSL GBs that undergo shear coupling. Fig. 13b(i) shows the scenario of  $\Sigma$ 13(320). 6 layers of successive (320) planes are pre-selected and colored differently. Because the interplanar spacing is much smaller than that of  $\Sigma 5(210)$ , more atoms are involved in each transformation unit. As the GB is passing through the pre-selected layers (Fig. 13b(ii)), atoms shuffle in a very complex but highly coordinated fashion, leading to gradual change in orientation of the transformation units. After the GB passes through, the units are reoriented and aligned with the bottom grain (Fig. 13b(iii)). However, after reorientation, each (320) plane remains single colored, for example, the cyan atoms, which have moved out of the units, remain on the same (320) plane that contains only cyan atoms. Similar analyses are also conducted for  $\Sigma$ 37(750) and  $\Sigma$ 13(510), and the results are provided in Supplemental Material.

GB structural units which are kites or diamonds or both at the GBs are also delineated in Fig. 12. The shapes of structural units change as the tilt angle varies, as analyzed and shown in numerous works [13,16,17,22,35,37,39,59,60]. Our analyses indicate that, irrespective of GB structural units, during shear coupling, lattice

transformation is accomplished in a very similar fashion: some GB atomic planes remain invariant and atoms on these planes are directly sheared to the lattice points of the neighboring grain, whereas the other GB atomic planes (non-invariant) swap their positions along the GB normal direction via highly coordinated shuffles. Thus, the interplanar spacing of the GB plane remains constant after lattice transformation. The GB structural units that enclose the GB free volume, only serve to provide the needed space for the highly coordinated shuffling to accomplish the lattice transformation.

Structural motifs, constructed by connecting lattice points that are invariantly sheared to the other grain were defined in [39] in which the first and second invariant planes were identified similarly to the present work. A major difference is that the motifs are not elemental, and how the other atoms that cannot be directly sheared to the lattice of the other grain is not resolved.

## 4.3. Kinetics of GB motion via shear coupling

The transformation units defined in this work allow development of a kinetics model for the migration of CSL GBs via shear coupling. Irrespective of GB type, the invariant plane, and the shape of GB free volume (either kite-like or other shapes), transfor-

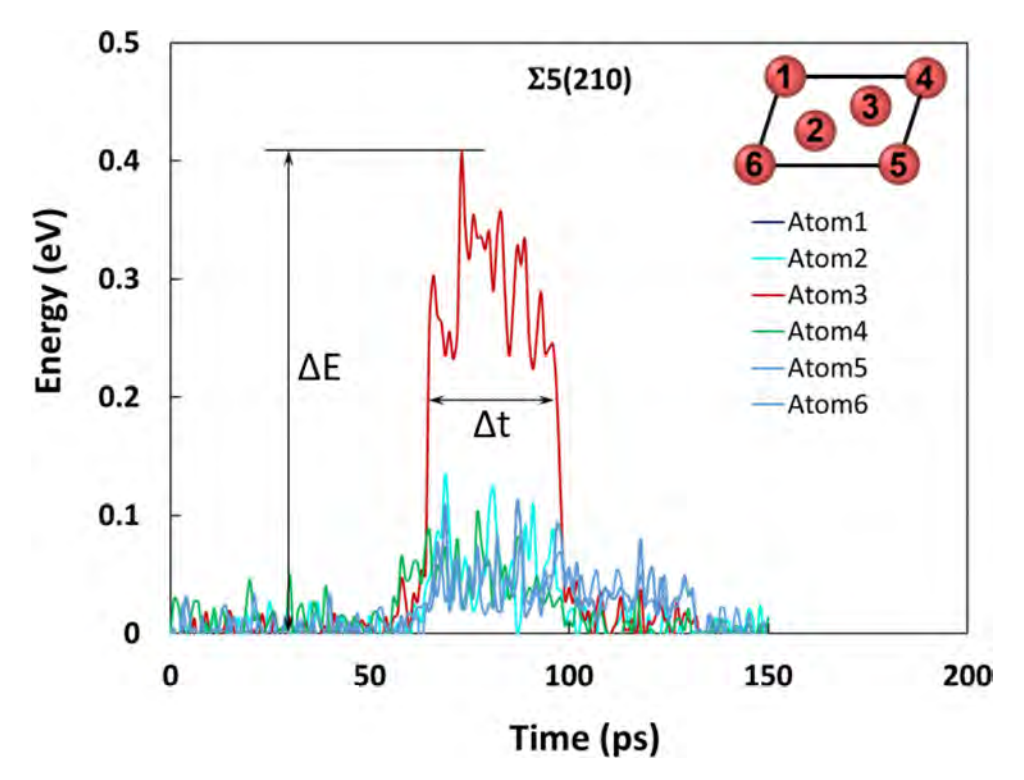


**Fig. 14.** Potential energy evolution of a group of six atoms in a transformation unit (the inset) in the case of  $\Sigma 5(210)$  during shear coupling. Atom 3 experiences the highest energy barrier,  $\Delta E$ , which is one of the rate-limiting factors. The other rate-limiting factor is the dwell time,  $\Delta t$ , which is the time needed for the transformation unit to complete its reorientation.

mation units can always be defined in a manner that is very similar to defining twinning elements in the classical twinning theory. Rate-limiting factors can now be identified.

The first rate-limiting factor is the number of atoms that are involved in the highly coordinated shuffling in a transformation unit during lattice reorientation, which is proportional to the area (A) of the unit. The migration velocity scales with  $\sqrt{A}$ . For CSL GBs in the form of  $\Sigma N(hk0)$  (N, h and k are integers) with the rotation axis of [001] and  $\{110\}$  invariant, the area A equals:

$$A = \frac{\sqrt{2}}{4} \sqrt{h^2 + k^2} \cdot a^2 \cdot \sin\alpha \tag{4}$$

where a is the lattice parameter. For those GBs with {100} invariant, the area A equals:

$$A = \frac{1}{4}\sqrt{h^2 + k^2} \cdot a^2 \cdot \sin\beta \tag{5}$$

The second rate-limiting factor is the energy barrier  $\Delta E$  for each transformation unit to overcome in completing its reorientation. The third rate-limiting factor is the dwell time  $\Delta t$ , which is the time that is needed to complete the coordinated shuffling. Both  $\Delta E$  and  $\Delta t$  can be obtained by analyzing the energy profiles of those atoms in the transformation unit, and an example of  $\Sigma 5(210)$  is provided in the following.

Fig. 14 shows the potential energy profiles of a group of six atoms in a transformation unit (four at the corners and two inside) in  $\Sigma5(210)$ . It can be seen that one of the atoms (Atom 3 in this case) experiences the highest energy barrier. Similar plots can be obtained for any other GBs that migrate via shear coupling. This highest energy barrier represents how difficult for the transformation unit to change the orientation, and thus corresponds to  $\Delta E$ . The dwell time  $\Delta t$  is simply the time that the atom experiencing the highest energy barrier stays at the high energy state during lattice transformation. After reorientation is completed, the energy drops back near the level before reorientation. The values of  $\sqrt{A}$ ,

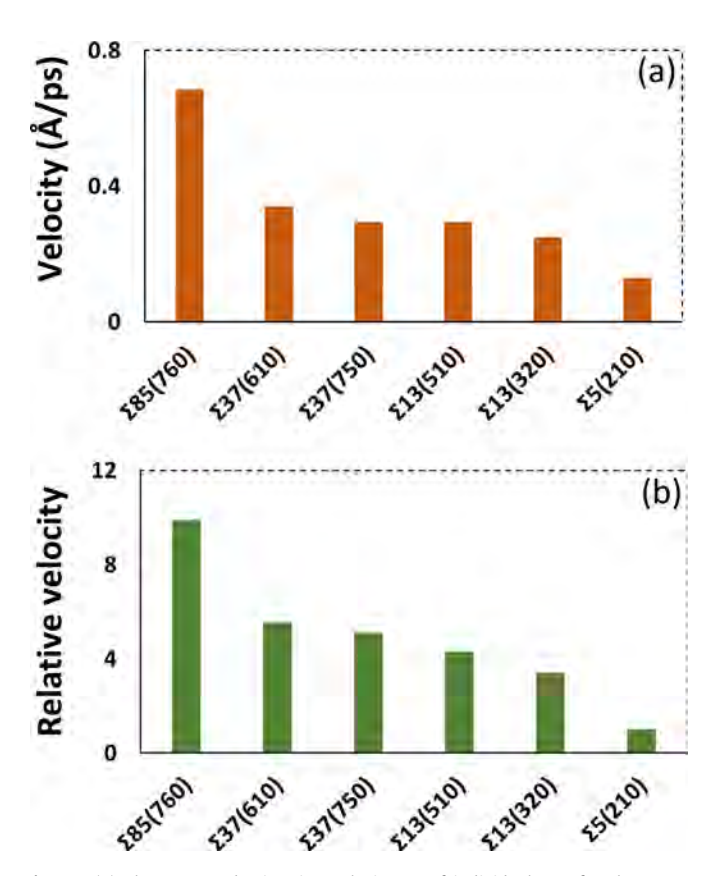


**Fig. 15.** (a) The measured migration velocity  $\nu_{\perp}$  of individual GBs for shear coupling. (b) Relative migration velocity of each GB plotted against the velocity of  $\Sigma 5(210)$ , calculated from Eq. (6). The overall trend in these two plots agrees reasonably well.

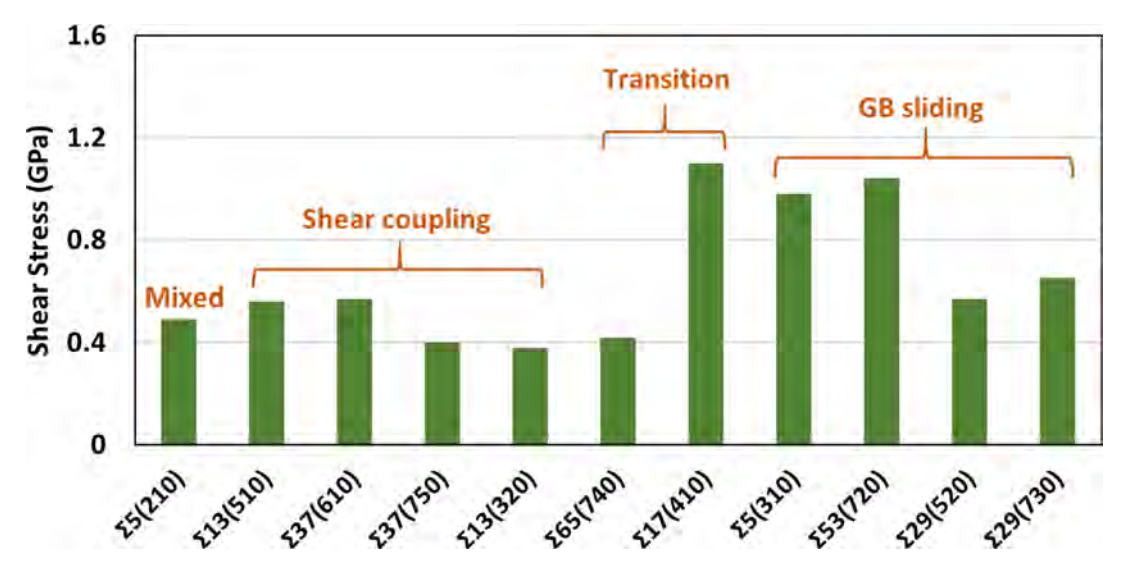


**Fig. 16.** The critical shear stresses for GBs that move by shear coupling, sliding and transition from shear coupling to sliding. In general, the critical shear stresses for sliding are considerably higher than those for shear coupling.  $\Sigma$ 65(740) and  $\Sigma$ 17(410) are in transition, but  $\Sigma$ 65(740) moves primarily by shear coupling, whereas  $\Sigma$ 17(410) moves primarily by sliding.

**Table 2**Values of the rate-limiting factors obtained from the simulations.

GB type	$\sqrt{A} \ (\mathring{A})$	$\Delta E$ (eV)	$\Delta t (ps)$
Σ85(760)	6.524	0.112	24
$\Sigma$ 37(610)	4.460	0.327	10
$\Sigma 37(750)$	6.261	0.357	14
$\Sigma 13(510)$	4.034	0.346	11
$\Sigma 13(320)$	4.107	0.351	14
$\Sigma 5(210)$	3.272	0.405	33

 $\Delta E$  and  $\Delta t$  for individual GBs that underwent shear coupling can be obtained from the simulation results and are listed in Table 2.

By combining all the rate-limiting factors, a general equation for the migration velocity of a GB by shear coupling can now be inferred based on the above analysis. At fixed external shear strain rate and temperature:

$$v_{\perp} = c \cdot \frac{\sqrt{A}}{\Delta t} \cdot \frac{k_B \cdot T}{\Delta E} \tag{6}$$

where c is the proportionality constant,  $k_B$  the Boltzmann constant and T the thermodynamic temperature.

To validate Eq. (6), firstly we re-plot the measured velocities of individual GBs in Fig. 9 into Fig. 15a. Then, we calculate the velocities of the GBs relative to that of  $\Sigma 5(210)$ , using the data in Table 2 and Eq. (6). The calculated results are plotted in Fig. 15b. If we compare these two plots, it can be seen that the overall trend agrees reasonably well. Note that Eq. (6) only contains quantities of geometry, energy barrier, and dwell time and they can be obtained from atomistic simulations. The measured velocities are also obtained from atomistic simulations and no experimental data are used for fitting. Inferring a more robust model is possible by taking into consideration mechanical energy which scales with  $\sigma\Omega$  ( $\sigma$  is the stress and  $\Omega$  the atomic volume) [22,61] during GB migration via shear coupling and fitting to experimentally acquired data.

Several other kinetics models were proposed by a number of researchers. Ivanov and Mishin [22] examined the effects of stress, velocity (shear strain rate) and temperature on shear coupling by using atomistic simulations and a model in which a particle was moved through a periodic potential was proposed. Effects of shear stress and temperature on shear coupling were also investigated by Chen et al. [15] and Han et al. [18] by assuming that GB migra-

tion was mediated by nucleation and glide of disconnections and a unified model was proposed, but how disconnections transform the lattice of one grain into the other was not considered in these models.

## 4.4. Why transition from shear coupling to sliding occurs at s $\approx 0.5$

Finally, we explain why transition from shear coupling to sliding occurs around  $s \approx 0.5$  (Fig. 8) for the GBs examined in this work. A possible reason is that a competition between shear coupling and GB sliding exists. To prove or disprove this point, the critical shear stresses for all the motion modes, including shear coupling and sliding, are computed. The average shear stress for each case is calculated over pre-selected mobile atoms in a region close to the top surface with known dimensions (thus the volume of the selected region is known) [48]. Ivanov and Mishin [22] showed that the virial stresses computed from the stress tensor of individual atoms were dependent of the size of the system. The location of selected region will also affect the calculated stresses. For consistency, the selected region is ~2 nm away from the fix top layer for all the GB cases.

The calculation results are shown in Fig. 16. It can be seen that generally the critical shear stresses for GB sliding are considerably higher than those for shear coupling. For  $\Sigma 65(740)$ , the motion mode is primarily shear coupling, and the critical stress is much lower than that for  $\Sigma 17(410)$  which moves primarily by sliding. Hence, in terms of critical shear stresses, GB sliding is always unfavorable for the GB types examined in this work, and it is unlikely that the transition from shear coupling to sliding is caused by the competition between the two motion modes.

Most likely, the transition is caused by the mismatch in the external strain rate and the strain rate produced by shear coupling. In our simulations, the top boundary layer is moving at a constant lateral velocity 0.1 Å/ps. The resultant external shear strain rate must be accommodated either by GB motion (via shear coupling or sliding) or dislocation slip in the matrix. If the lateral migration velocity  $v_{\parallel}$  by shear coupling is slower than 0.1 Å/ps, then sliding or dislocation nucleation and glide will occur. Indeed, dislocation glide can be observed in the cases of sliding, for example, Fig. 2b and 3b. For  $\Sigma 5(210)$ , the vertical velocity  $v_{\perp}$  equals 0.13 Å/ps, and this gives the lateral velocity  $v_{\parallel}$  about 0.08 Å/ps because  $\frac{v_{\perp}}{v_{\parallel}} = \frac{1}{2}tan\alpha$  [13]. This lateral velocity is insufficient to com-

pensate the external shear strain rate. As a result, part of the  $\Sigma5(210)$  GB moves by shear coupling, whereas the other parts of the GB move by sliding (Figs. 10-11). A similar scenario can be seen for  $\Sigma65(740)$ . The vertical velocity  $v_{\perp}$  equals 0.17 Å/ps, and this gives the lateral velocity  $v_{\parallel}$  about 0.09 Å/ps which is slightly short to match the external shear strain rate. Accordingly, this GB moves mostly by shear coupling, but sliding occurs and disrupts shear coupling intermittently (Fig. 4e). For all other GBs that move by shear coupling, the lateral velocity is above 0.1 Å/ps, and thus their motion is dominated solely by shear coupling.

If the external shear strain rate is reduced, transition from shear coupling to sliding still occurs. This is because similar energy barrier and critical shear stress must be overcome, irrespective of the shear strain rate. As the shear strain rate slows down, the GB migration velocity slows down accordingly. Indeed, for  $\Sigma$ 17(410), when the shear strain rate is reduced by a factor of 5, the GB motion is still dominated by sliding. For  $\Sigma$ 65(740), when the shear strain rate is reduced by half, GB sliding still occurs and disrupts shear coupling.

Transition from shear coupling to sliding due to temperature increase was observed and discussed by Cahn et al. [13]. As the simulation temperature increases to a certain value, the fraction of sliding in each CSL GB suddenly jumps. The transition was attributed to the crossover of the respective critical stresses. Han et al. [18] attributed such temperature-dependent transition to nucleation and glide of different disconnections on GBs.

#### 5. Conclusions

In this work, novel structural analyses were conducted to reveal how the lattice of a grain is transformed to that of a neighboring grain during migration via shear coupling of CSL GBs with a tilting axis of [001] in FCC Cu under shear loading parallel to the GB plane. The following conclusions can be reached based on the simulation results:

- (1) Very similar to the magnitude of twinning shear, the angles between the invariant plane, i.e. either  $\{100\}$  or  $\{110\}$ , and the GB plane can be used to define a structural factor "magnitude of shear" s, which largely determines the mode of motion and migration velocity of the GBs. The migration velocity via shear coupling increases with decreasing s. Approximately, when one of the two invariant planes has s < 0.5, shear coupling occurs; when 0.5 < s < 0.6, shear coupling transitions to GB sliding; when both invariant planes have s > 0.6, GB sliding occurs. Such a transition occurs when the migration velocity via shear coupling is insufficient to accommodate the external shear strain rate.
- (2) For all the CSL GBs that migrate via shear coupling, irrespective of their type, invariant plane and GB structure, some GB atomic planes remain invariant, and these planes can be defined as invariant plane as well, in a manner very similar to the definition of the first invariant plane in deformation twinning. This allows definition of transformation units in various CSL GBs. Atoms in the transformation units shuffle in a highly coordinated fashion, such that the other GB atomic planes swap their positions along the GB normal direction, leading to reorientation of the units toward the neighboring grain. This behavior ensures that no volumetric dilation or contraction occurs along the GB normal direction.
- (3) Rate-limiting factors for shear coupling, i.e. the geometry of transformation unit, the energy barrier for lattice transformation, and the time for completing the reorientation of the unit, are identified. These factors can be used to derive a more physical model to describe the kinetics of GB migration via shear coupling.

## **Declaration of Competing Interest**

The authors declare that they have no known competing financial interests or personal relationships that could have appeared to influence the work reported in this paper.

#### Acknowledgements

Bin Li gratefully thanks the support from U.S. National Science Foundation (CMMI-1635088 and 2016263).

#### Supplementary materials

Supplementary material associated with this article can be found, in the online version, at doi:10.1016/j.actamat.2021.117127.

#### References

- [1] H. Fukutomi, T. Kamijo, Grain boundary sliding-migration of aluminum <110> Σ11 {113} symmetric tilt coincidence grain boundary and its interpretation based on the motion of perfect DSC dislocations, Scr. Metall. 19 (1985) 195– 197, doi:10.1016/0036-9748(85)90181-4.
- [2] H. Fukutomi, T. Iseki, T. Endo, T. Kamijo, Sliding behavior of coincidence grain boundaries deviating from ideal symmetric tilt relationship, Acta Metall. Mater. 39 (1991) 1445–1448, doi:10.1016/0956-7151(91)90229-T.
- [3] D.A. Molodov, V.A. Ivanov, G. Gottstein, Low angle tilt boundary migration coupled to shear deformation, Acta Mater. 55 (2007) 1843–1848, doi:10.1016/j. actamat.2006.10.045.
- [4] D.A. Molodov, T. Gorkaya, G. Gottstein, Mechanically driven migration of <100&gt; tilt grain boundaries in Al-bicrystals, Mater. Sci. Forum. (2007), doi:10.4028/www.scientific.net/MSF.558-559.927.
- [5] D.A. Molodov, T. Gorkaya, G. Gottstein, Dynamics of grain boundaries under applied mechanical stress, J. Mater. Sci. 46 (2011) 4318–4326, doi:10.1007/ s10853-010-5233-6.
- [6] D.A. Molodov, T. Gorkaya, G. Gottstein, Migration of the Σ7 tilt grain boundary in Al under an applied external stress, Scr. Mater. 65 (2011) 990–993, doi:10. 1016/j.scriptamat.2011.08.030.
- [7] K.D. Molodov, D.A. Molodov, Grain boundary mediated plasticity: on the evaluation of grain boundary migration - shear coupling, Acta Mater. 153 (2018) 336–353, doi:10.1016/j.actamat.2018.04.057.
- [8] F. Mompiou, D. Caillard, M. Legros, Grain boundary shear-migration coupling— I. In situ TEM straining experiments in Al polycrystals, Acta Mater. 57 (2009) 2198–2209, doi:10.1016/j.actamat.2009.01.014.
- [9] T. Gorkaya, D.A. Molodov, G. Gottstein, Stress-driven migration of symmetrical <100> tilt grain boundaries in Al bicrystals, Acta Mater. 57 (2009) 5396–5405, doi:10.1016/j.actamat.2009.07.036.
- [10] T. Gorkaya, K.D. Molodov, D.A. Molodov, G. Gottstein, Concurrent grain boundary motion and grain rotation under an applied stress, Acta Mater. 59 (2011) 5674–5680, doi:10.1016/j.actamat.2011.05.042.
- [11] G. Gottstein, D.A. Molodov, L.S. Shvindlerman, Grain boundary migration in metals: recent developments, Interface Sci. 6 (1998) 7–22, doi:10.1023/A: 1008641617937.
- [12] M. Winning, In-situ observations of coupled grain boundary motion, Philos. Mag. 87 (2007) 5017–5031, doi:10.1080/14786430701601759.
- [13] J.W. Cahn, Y. Mishin, A. Suzuki, Coupling grain boundary motion to shear deformation, Acta Mater. 54 (2006) 4953–4975, doi:10.1016/j.actamat.2006.08.
- [14] D.G. Brandon, The structure of high-angle grain boundaries, Acta Metall. 14 (1966) 1479–1484, doi:10.1016/0001-6160(66)90168-4.
- [15] K. Chen, J. Han, S.L. Thomas, D.J. Srolovitz, Grain boundary shear coupling is not a grain boundary property, Acta Mater. 167 (2019) 241–247, doi:10.1016/j. actamat.2019.01.040.
- [16] K. Cheng, L. Zhang, C. Lu, K. Tieu, Coupled grain boundary motion in aluminium: the effect of structural multiplicity, Sci. Rep. 6 (2016) 1–11, doi:10.1038/srep25427.
- [17] Y. Deng, C. Deng, Size and rate dependent grain boundary motion mediated by disconnection nucleation, Acta Mater. 131 (2017) 400–409, doi:10.1016/j. actamat.2017.04.018.
- [18] J. Han, S.L. Thomas, D.J. Srolovitz, Grain-boundary kinetics: a unified approach, Prog. Mater. Sci. 98 (2018) 386-476, doi:10.1016/j.pmatsci.2018.05.004.
- [19] E.R. Homer, High-throughput simulations for insight into grain boundary structure-property relationships and other complex microstructural phenomena, Comput. Mater. Sci. 161 (2019) 244–254, doi:10.1016/j.commatsci.2019.01. 041.
- [20] E.R. Homer, S.M. Foiles, E.A. Holm, D.L. Olmsted, Phenomenology of shear-coupled grain boundary motion in symmetric tilt and general grain boundaries, Acta Mater. 61 (2013) 1048–1060, doi:10.1016/j.actamat.2012.10.005.
- [21] J. Humberson, I. Chesser, E.A. Holm, Contrasting thermal behaviors in Σ3 grain boundary motion in nickel, Acta Mater. 175 (2019) 55–65, doi:10.1016/j.actamat.2019.06.003.

[22] V.A. Ivanov, Y. Mishin, Dynamics of grain boundary motion coupled to shear deformation: an analytical model and its verification by molecular dynamics, Phys. Rev. B. 78 (2008) 064106, doi:10.1103/PhysRevB.78.064106.

- [23] H.A. Khater, A. Serra, R.C. Pond, J.P. Hirth, The disconnection mechanism of coupled migration and shear at grain boundaries, Acta Mater. 60 (2012) 2007– 2020, doi:10.1016/j.actamat.2012.01.001.
- [24] K. McReynolds, K.-A. Wu, P. Voorhees, Grain growth and grain translation in crystals, Acta Mater. 120 (2016) 264–272, doi:10.1016/j.actamat.2016.08.056.
- [25] D.L. Olmsted, E.A. Holm, S.M. Foiles, Survey of computed grain boundary properties in face-centered cubic metals—II: grain boundary mobility, Acta Mater. 57 (2009) 3704–3713, doi:10.1016/j.actamat.2009.04.015.
- [26] J.L. Priedeman, D.L. Olmsted, E.R. Homer, The role of crystallography and the mechanisms associated with migration of incoherent twin grain boundaries, Acta Mater. 131 (2017) 553–563, doi:10.1016/j.actamat.2017.04.016.
- [27] A. Rajabzadeh, F. Mompiou, M. Legros, N. Combe, Elementary mechanisms of shear-coupled grain boundary migration, Phys. Rev. Lett. 110 (2013) 265507, doi:10.1103/PhysRevLett.110.265507.
- [28] A.D. Sheikh-Ali, Coupling of grain boundary sliding and migration within the range of boundary specialness, Acta Mater. 58 (2010) 6249–6255, doi:10.1016/ i.actamat.2010.07.043
- [29] A.D. Sheikh-Ali, R.Z. Valiev, Dislocation analysis of the coupling of grain boundary sliding and migration during the deformation of Zn bicrystals, Phys. Status Solidi A. 117 (1990) 429–436, doi:10.1002/pssa.2211170212.
- [30] S.L. Thomas, K. Chen, J. Han, P.K. Purohit, D.J. Srolovitz, Reconciling grain growth and shear-coupled grain boundary migration, Nat. Commun. 8 (2017) 1–12, doi:10.1038/s41467-017-01889-3.
- [31] Z.T. Trautt, Y. Mishin, Grain boundary migration and grain rotation studied by molecular dynamics, Acta Mater. 60 (2012) 2407–2424, doi:10.1016/j.actamat. 2012.01.008.
- [32] L. Wan, S. Wang, Shear response of the \${upSigma, Modelling Simul. Mater. Sci. Eng. 17 (2009) 045008, doi:10.1088/0965-0393/17/4/045008.
- [33] J. Wang, A. Misra, J.P. Hirth, Shear response of \$\ensuremath{\sigma}3{112}\$ twin boundaries in face-centered-cubic metals, Phys. Rev. B. 83 (2011) 064106, doi:10.1103/PhysRevB.83.064106.
- [34] H. Zhang, D. Du, D.J. Srolovitz, Effects of boundary inclination and boundary type on shear-driven grain boundary migration, Philos. Mag. 88 (2008) 243– 256, doi:10.1080/14786430701810764.
- [35] L. Zhang, C. Lu, G. Michal, K. Tieu, K. Cheng, Molecular dynamics study on the atomic mechanisms of coupling motion of [0 0 1] symmetric tilt grain boundaries in copper bicrystal, Mater. Res. Express. 1 (2014) 015019, doi:10. 1088/2053-1591/1/1/015019.
- [36] A. Adland, A. Karma, R. Spatschek, D. Buta, M. Asta, Phase-field-crystal study of grain boundary premelting and shearing in bcc iron, Phys. Rev. B. 87 (2013) 024110, doi:10.1103/PhysRevB.87.024110.
- [37] Z.T. Trautt, A. Adland, A. Karma, Y. Mishin, Coupled motion of asymmetrical tilt grain boundaries: molecular dynamics and phase field crystal simulations, Acta Mater. 60 (2012) 6528–6546, doi:10.1016/j.actamat.2012.08.018.
- [38] B. Li, P.C. Clapp, J.A. Rifkin, X.M. Zhang, Molecular dynamics calculation of heat dissipation during sliding friction, Int. J. Heat Mass Transf. 46 (2003) 37–43, doi:10.1016/S0017-9310(02)00258-2.
- [39] D. Caillard, F. Mompiou, M. Legros, Grain-boundary shear-migration coupling. II. Geometrical model for general boundaries, Acta Mater. 57 (2009) 2390–2402, doi:10.1016/j.actamat.2009.01.023.
- [40] R.E. Reed-Hill, Physical Metallurgy Principles, (The... book by Robert E. Reed-Hill, 1992.

- [41] J.W. Christian, S. Mahajan, Deformation twinning, Prog. Mater. Sci. 39 (1995) 1–157, doi:10.1016/0079-6425(94)00007-7.
- [42] M. Niewczas, Lattice correspondence during twinning in hexagonal close-packed crystals, Acta Mater. 58 (2010) 5848–5857, doi:10.1016/j.actamat.2010. 06.059
- [43] B. Li, Y. Shen, Q. An, Structural origin of reversible martensitic transformation and reversible twinning in NiTi shape memory alloy, Acta Mater. 199 (2020) 240–252, doi:10.1016/j.actamat.2020.08.039.
- [44] J.W. Cahn, Y. Mishin, A. Suzuki, Duality of dislocation content of grain boundaries, Philos. Mag. 86 (2006) 3965–3980, doi:10.1080/14786430500536909.
- [45] Y. Mishin, M.J. Mehl, D.A. Papaconstantopoulos, A.F. Voter, J.D. Kress, Structural stability and lattice defects in copper: ab initio, tight-binding, and embeddedatom calculations, Phys. Rev. B. 63 (2001) 224106, doi:10.1103/PhysRevB.63. 224106.
- [46] W.G. Hoover, Canonical dynamics: equilibrium phase-space distributions, Phys. Rev. A. 31 (1985) 1695–1697, doi:10.1103/PhysRevA.31.1695.
- [47] S. Nosé, A unified formulation of the constant temperature molecular dynamics methods, J. Chem. Phys. 81 (1984) 511–519, doi:10.1063/1.447334.
- [48] S. Plimpton, Fast Parallel Algorithms for Short-Range Molecular Dynamics, J. Comput. Phys. 117 (1995) 1–19, doi:10.1006/jcph.1995.1039.
- [49] B.A. Bilby, A.G. Crocker, The Theory of the Crystallography of Deformation Twinning, Proc. R. Soc. Lond. Ser. Math. Phys. Sci. 288 (1965) 240–255, doi:10. 1098/rspa.1965.0216.
- [50] B. Li, P.C. Clapp, J.A. Rifkin, X.M. Zhang, Molecular dynamics simulation of stick-slip, J. Appl. Phys. 90 (2001) 3090–3094, doi:10.1063/1.1394916.
- [51] J.W. Cahn, J.E. Taylor, A unified approach to motion of grain boundaries, relative tangential translation along grain boundaries, and grain rotation, Acta Mater. 52 (2004) 4887–4898, doi:10.1016/j.actamat.2004.02.048.
- [52] J.W. Christian, The Theory of Transformations in Metals and Alloys, Newnes,
- [53] B. Li, H. El Kadiri, M.F. Horstemeyer, Extended zonal dislocations mediating twinning in titanium, Philos. Mag. 92 (2012) 1006–1022, doi:10.1080/14786435.2011.637985.
- [54] A. Serra, D.J. Bacon, Modelling the motion of {1122} twinning dislocations in the HCP metals, Mater. Sci. Eng. A. 400–401 (2005) 496–498, doi:10.1016/j. msea.2005.01.067.
- [55] A. Stukowski, Visualization and analysis of atomistic simulation data with OVITO-the Open Visualization Tool, Model. Simul. Mater. Sci. Eng. 18 (2010) 015012. doi:10.1088/0965-0393/18/1/015012.
- [56] N. Thompson, D.J. Millard, XXXVIII. Twin formation, in cadmium, Philos. Mag. Ser. 7. 43 (1952) 422-440, doi:10.1080/14786440408520175.
- [57] B. Li, E. Ma, Zonal dislocations mediating {10-11}<10-1-2>twinning in magnesium, Acta Mater. 57 (2009) 1734-1743, doi:10.1016/j.actamat.2008.12.016.
- [58] S. Mendelson, Zonal dislocations and twin lamellae in h.c.p. metals, Mater. Sci. Eng. 4 (1969) 231–242, doi:10.1016/0025-5416(69)90067-6.
- [59] N. Combe, F. Mompiou, M. Legros, Disconnections kinks and competing modes in shear-coupled grain boundary migration, Phys. Rev. B. 93 (2016) 024109, doi:10.1103/PhysRevB.93.024109.
- [60] X.Y. Sun, C. Fressengeas, V. Taupin, P. Cordier, N. Combe, Disconnections, dislocations and generalized disclinations in grain boundary ledges, Int. J. Plast. 104 (2018) 134–146, doi:10.1016/j.ijplas.2018.02.003.
- [61] T.H. Courtney, Mechanical Behavior of Materials, 2 edition, Waveland Pr Inc, 2005.